FLEET TECHNOLOGY LIMITED

HEAT-AFFECTED ZONE TOUGHNESS OF SHIP PLATE

Final Report

by:

N. Pussegoda and L. Malik

Work on this project was carried out under the auspices of the Canada Centre for Mineral and Metallurgical Technology and Panel for Energy Research and Development (PERD).

DSS Contract No. : 23440-1-9158/01-SQ

DSS File No. : 034SQ.23440-1-9158

CANMET Project No. : 1-9158

Scientific Authority : Dr. W. Tyson

37 pp

March 1992

MICROMEDIA

EXECUTIVE SUMMARY

This study was performed to complete the toughness characterization of the weld heat-affected zone (HAZ) of the WP steel plate which conforms to ABS Grade DH36 (ship steel) requirements. The weld represented typical shipyard practice for mechanized submerged arc welds of 25 mm thick plate, i.e., two passes using relatively high heat input of about 5.5 kJ/mm.

Previous work assessed the crack arrest behaviour and the nil-ductility transition (NDT) temperature of the HAZ described above. The present work therefore was aimed to determine the CTOD toughness of the grain-coarsened HAZ. Another objective was to determine the sensitivity of the less expensive CVN test to the GCHAZ.

In the CTOD test, when unstable fracture initiated from regions where the prior austenite grain size was about 150 μm, low values (i.e., $\delta_c < 0.2$ mm) were produced up to a test temperature of 40°C. When fractures initiate outside the GCHAZ, the CTOD values are significantly higher at temperatures above -20°C. On the other hand, below -20°C, the CTOD values are similar for both regions. The CVN test results also displayed a higher transition temperature for the GCHAZ compared to the CVN curve obtained from specimens representing fractures outside the GCHAZ region. However, the shift in the 40 J transition temperature was smaller than that in the 0.1 mm CTOD transition temperature.

It is suggested that a fracture control plan based solely on HAZ CTOD toughness could be too conservative and expensive, and the one based on the crack arrest toughness of base materials and HAZ could be more economical.

SOMMAIRE

Cette étude a été réalisée pour compléter la caractérization de la zone affectée thermiquement (ZAT) d'une soudure d'une plaque d'acier WP, acier qui est conforme aux exigences de la nuance DH36 des normes ABS (acier naval). La soudure représentait une pratique typique des constructeurs navals pour la soudage mécanisé à l'arc submergé de plaques de 25 mm d'épaisseur, i.e. deux passes utilisant un apport calorifique élevé d'environ 5.5 kJ/mm.

Les travaux précédents évaluaient le comportement à l'arrét de fissure et la température de transition de ductilité nulle (NDT) de la ZAT décrite plus haut. Le présent ouvrage par conséquent avait pour but de déterminer la ténacité (CTOD) des grains grossiers de la ZAT. Un autre objectif a été de déterminer la sensibilité de l'essai Charpy, moins coûteux, aux grains grossiers de la ZAT.

Dans l'essai de CTOD, lorsqu'une rupture instable s'initiait d'une région où les grains antérieurs de l'austénite étaient d'environ 150 µm, de faible valeurs (i.e. $\delta_c < 0.2$ mm) ont été obtenues, et ce, jusqu'à des température d'essai de 40°C. Lorsque la rupture s'initait en dehors de la ZAT à grains grossiers, les valeurs de CTOD ont été significativement plus élevées, et ce, pour des températures supérieures à -20°C. D'un autre côté, en dessous de -20°C, les valeurs de CTOD ont été similaires pour les deux régions. Les résultats des essais Charpy (CVN) ont aussi montrés une température de transition plus élevées pour la ZAT à gros grains comparé à la courbe CVN obtenue des spécimens pris à l'extérieur de cette région. Cependant, le changement dans la température de transition de 40 J était plus petit que celui de la température de transition du CTOD à 0.1 mm.

Il est suggéré qu'un plan de contrôle de rupture basé exclusivement sur la ténacité (CTOD) de la ZAT pourrait être trop conservateur et coûteux, et qu'un plan basé sur la ténacité à l'arrêt de fissure du matériel de base et de la ZAT pourrait être plus économique.

TABLE OF CONTENTS

Page

EXECUTIVE SUMMARY

SOMMAIRE

1.0 INTRODUCTION 1

2.0 EXPERIMENTAL METHODS 2

2.1 WELDING OF PANELS 2
2.2 HARDNESS MEASUREMENTS 2
2.3 MACHINING OF STANDARD B X 2B CTOD SPECIMENS 3
2.4 CTOD TESTING 3
2.5 POST-TEST METALLOGRAPHY OF BROKEN CTOD SPECIMENS . 4
2.6 MACHINING AND TESTING CVN SPECIMENS 4

3.0 RESULTS AND DISCUSSION 5

3.1 MACROSTRUCTURE AND HARDNESS CHARACTERIZATION OF THE WELD 5
3.2 CTOD RESULTS 5
3.3 ANALYSIS OF THE CTOD RESULTS 7
3.4 CVN RESULTS 8
3.5 SIGNIFICANCE OF THE RESULTS 8

4.0 CONCLUSIONS 9

5.0 REFERENCES 10

TABLES AND FIGURES

1.0 INTRODUCTION

In a previous project (1) carried out on behalf of the Metals Technology Laboratories, CANMET and the Canadian Coast Guard, the brittle fracture initiation toughness at quasi-static and intermediate (representing mid-ship region) strain rates has been studied for a number of ship steels. Their plane strain crack arrest toughness and their nil-ductility transition (NDT) temperatures were also determined (1).

The weld heat-affected zone (HAZ) in one of the steels, designated as WP, was subsequently characterized in another investigation (2). The 25 mm thick WP steel plate was welded in two passes using a relatively high heat input of about 5.5 kJ/mm, typical of ship yard practice for mechanized submerged arc welds. Based on the processing route, chemistry, tensile and Charpy V-notch properties, the WP steel plate conformed to ABS grade DH36 requirements. The HAZ of the weld described above was also assessed to determine its NDT temperature and crack arrest behaviour using the short crack arrest and plain strain crack arrest test procedures.

The structural welding codes for ships generally do not require any assessment of the HAZ toughness, even though it is well known that the grain-coarsened regions of the HAZ represent 'local brittle zones' (LBZs). A recent study (3) has demonstrated that these can trigger brittle fracture initiation, and then the crack arrest toughness of the surrounding regions and the base material are the critical properties from the point of view of the integrity of the structure.

As the crack arrest performance of the WP base plate and HAZ has been assessed (2), this study aims to determine the CTOD toughness of the same HAZ to develop a complete characterization of the HAZ toughness properties. Another objective is to determine the sensitivity of the less expensive CVN test to LBZs that might be present in the HAZ.

2.0 EXPERIMENTAL METHODS

2.1 WELDING OF PANELS

The main objective of this task was to make welded panels that can be used to machine CTOD specimens. The welding procedures developed previously (2) and employed here for making these panels is given in Table 1, and it had the objectives of:

(a) employing a relatively high heat input, two pass welding procedure, typical of shipyard practice for machine (mechanized submerged arc) welds;

(b) producing a relatively straight HAZ; this was achieved by selecting a machined groove of the design shown in Table 1 and by using a bar at the top to reduce the extent of capping pass nail head.

A typical cross-section of the weld is shown in Figure 1.

The welding consumables used were:

Lincoln LA75 wire (5 mm diameter)
Lincoln 880M flux

The wire contains nominally 1% nickel and supplier's technical literature indicates that weld metal toughness should at least meet the requirement of 40 J at -50°C in the as-welded condition (using the standard test procedure outlined in CSA Standard W48.6).

All welds were made perpendicular to the rolling direction so that the fracture path in the HAZ would also be perpendicular to the rolling direction, as was the case with the CTOD, compact crack arrest and NDT tests in the base material (1). The same fracture path orientation was maintained for the compact crack arrest (CCA) and NDT test used to assess the HAZ (2).

2.2 HARDNESS MEASUREMENTS

Two representative cross sections of the weld were prepared to perform Vickers hardness traverses using a 5 kg load. These traverses were done at the subsurface and half-thickness locations.

2.3 MACHINING OF STANDARD B X 2B CTOD SPECIMENS

The following procedure was adopted:

i) Oversize blanks were removed from the weld panels so that the specimen length is exactly normal to the weld.

ii) Each specimen was macro-etched on both weld ends using 10% nital to delineate the fusion line and check the HAZ straightness.

iii) The weld reinforcement was machined off and the specimens were squared to the final B X 2B dimensions.

iv) Finally, the specimens were macro-etched on both ends and lines were scribed on both weld ends to maximize the intersection with the GCHAZ. Machine notches were then placed in the through-thickness orientation.

2.4 CTOD TESTING

The recommendations of Towers and Robinson (4) were followed with the aim of reducing uneven fatigue crack growth experienced frequently during pre-cracking of weld specimens. This was done by locally compressing a part of the ligament ahead of the machined notch by 0.5% on each side of the specimen. This procedure is believed to reduce the variation in residual stresses and aid the uniform growth of the fatigue crack. Fatigue pre-cracking was performed according to BS 5762.

The pre-cracked specimens were fully immersed in a well-stirred alcohol bath cooled by liquid nitrogen. The temperature was measured by a calibrated thermocouple, spot welded to the specimen in the vicinity of the fatigue crack. The accuracy of the temperature control set up was within ± 2°C. The specimen was maintained at the selected test temperature for a minimum of 10 minutes before performing the test according to BS 5762. All the tests were carried out at a quasi-static loading rate obtained by the cross head moving rate of 0.0127 mm s^{-1}. Subsequent to the termination of the test the specimens were broken completely to observe the fracture faces and determine the effective crack depths. These observations are necessary to determine the validity of the test results and for assessing the failure mode (BS 5762).

During the early stages of testing, most specimens produced brittle fractures, displaying coarse shiny facets representative of the grain-coarsened HAZ (GCHAZ), without any stable crack growth below the fatigue crack front. The load vs. clip gauge displacement plots displayed limited plasticity confirming this behaviour. Due to the low toughness of the GCHAZ at room temperature, some tests were also performed

above the room temperature by immersing the specimens in hot water. As it was also desirable to obtain fracture toughness of the HAZ excluding the LBZs in some specimens, the notches were placed ≈ 0.5 to 1 mm from the fusion boundary as to avoid intersection with the GCHAZ. The notches in all cases were still within the etched HAZ.

2.5 POST-TEST METALLOGRAPHY OF BROKEN CTOD SPECIMENS

The broken half of the CTOD specimen containing the weld is selected for this analysis. The fracture faces were removed from this half of the specimen and they were used to produce two sections, both normal to the fracture face, for metallography as follows:

i) One, immediately behind the fatigue crack front to establish the proportion of various microstructural regions sampled by the fatigue crack;

ii) The second, through the brittle fracture initiation site to establish the associated microstructure.

2.6 MACHINING AND TESTING CVN SPECIMENS

Standard (10 mm x 10 mm x 55 mm) specimens were extracted approximately at the quarter thickness location, where the V-notch could be placed in GCHAZ (see Figure 1). The notch is positioned in the through thickness direction and the specimen length is perpendicular to the weld; the fracture path orientation was thus consistent with the CTOD tests and previous work (1,2).

As in the case of CTOD specimens, the location for the placement of the V-notch of each specimen was marked after macro etching. Here a line was scribed as close as possible to the fusion line to maximize the length that intersects with the GCHAZ. The tests were carried out over a temperature range with the aim of determining the transition curves for the GCHAZ and the remaining region of the HAZ.

3.0 RESULTS AND DISCUSSION

3.1 MACROSTRUCTURE AND HARDNESS CHARACTERIZATION OF THE WELD

Figure 1 displays the typical weld cross section macro-structure and shows a relatively large straight GCHAZ associated with the second pass. Table 2 presents the hardness of the parent metal, GCHAZ and the weld metal obtained from traverses carried out along the subsurface (Side 2) and half-thickness locations. The results show that the weld metal and GCHAZ have similar hardness and they are greater than the base metal value.

3.2 CTOD RESULTS

The fracture face examination and post-test metallography produced two important observations:

i) The fatigue crack front was relatively straight, i.e., it displayed almost no curvature; therefore all the test results were valid according to BS 5762.

ii) All of the fractures that showed coarse shiny facets in the initiating regions can be associated with the GCHAZ of the weld.

iii) When the initiating regions contain coarse shiny facets, the identification of the exact site is more difficult than when initiation occurs outside the GCHAZ, thus presenting a relatively darker fracture.

The observation i) above shows that the pre-compression suggested by Towers and Robinson (4) has been effective in reducing the possibility of uneven fatigue crack growth due to non-uniform residual stresses usually present in welds. The CTOD results presented in Table 3, are grouped separately depending on the brittle fracture initiation site, i.e., GCHAZ or the surrounding HAZ.

All of the CTOD values representing the GCHAZ except for the test carried out at the highest test temperature (46°C) fractured *before* the onset of slow stable crack growth; thus CTOD's are recorded as (δ_c) values. In contrast, at 46°C, the unstable fracture occurred *after* the onset of slow crack growth, and therefore the CTOD is recorded as (δ_u) value.

To calculate the above CTOD's the GCHAZ yield strength has to be estimated, and this was done using a relationship between the 0.2% off set yield strength and hardness (5). Accordingly, the ambient temperature yield strength was estimated to be 405 MPa and is higher than the base metal yield strength of 375 MPa. For convenience,

the CTOD's of the fractures occurring outside the GCHAZ was also calculated using 405 MPa. In the latter case, the errors will be negligible because the yield strength is used only for the determination of the elastic component of the CTOD; as most fractures occurred after slow crack growth the significant contribution is from the plastic component. More importantly, the temperature dependence of the yield strength was taken into account using Irwin's relationship (6) given below (see Table 3).

$$\sigma_y = 405 + \frac{10^5}{491 + 1.8T} - 189 \qquad (1)$$

where σ_y is the yield strength (MPa) at the test temperature (T °C).

Based on post-test metallography, the position of the fatigue crack front in relation to the fusion line can be separated into the following categories:

i) In most of the specimens the entire fatigue crack front is in the HAZ, and a large portion (> 15%) of the front falls in the GCHAZ (≥ 100 μm).

ii) Eight specimens had a portion of the fatigue crack front placed in the weld metal; however, this portion was small or near the specimen surface, and the brittle fracture initiation still occurred in the GCHAZ.

iii) In four specimens the interaction with the GCHAZ was less than 10% of its length and all of these were notched intentionally to avoid the GCHAZ.

In most of the cases described in i) above, the unstable brittle fracture initiated close to the fusion line, in the GCHAZ (Figures 2 to 4). However, in three specimens (I.D.s 1-1, 1-3 and 2-7) that fall into this category, the unstable fractures were *not* initiated from the GCHAZ. Two of these are shown in Figures 5 and 6. When the machined notch was placed deliberately outside the GCHAZ (category iii), fracture initiation *always* occurred outside the GCHAZ (see Figure 7). All eight test specimens in category ii) had their fracture initiation sites located in the GCHAZ, see Figures 8 and 9.

On a percentage basis, if the fatigue crack sampled sufficient GCHAZ, (>15% of its length) or interacted with the fusion line, only 13%, i.e. 3 out of 23 specimens, produced fractures initiating outside the GCHAZ. This behaviour can be expected, because in this two pass weld most of the region adjacent to the fusion line is GCHAZ;

in contrast, in multi-pass welds, a significant portion of this region is refined by the subsequent passes.

Figures 8 and 9 demonstrate that portions of the fatigue crack front that fall in the weld metal jump to the fusion line/GCHAZ once the unstable fracture is initiated; compare macrographs 8(a) and 9(a) that display the fatigue crack front with 8(b) and 9(b), respectively, showing a cross section of the fracture initiation plane.

In Table 3, the CTOD results have been separated based on the initiated site being in the GCHAZ or outside. The aimed location for placing the notch is also indicated in the table for each specimen. Examination of the fracture surfaces and the metallographically-prepared cross-sections confirmed that coarse shiny facets on the fracture surface were associated with grain-coarsened HAZ, typically greater that 100 μm (Figures 10(a) and (b), for example). In contrast, Figure 11 pertains to a specimen wherein stable crack growth occurred outside the GCHAZ. The fracture face (Figure 11(a)) displays the ductile extension before unstable fracture initiated from an area representing fine dull facets, compared to the coarse shiny facets in Figure 10(a). The macrograph of the cross-section taken at the unstable fracture initiation plane shows that initiation occurred outside the GCHAZ.

Typical photomicrographs representing fracture initiation regions from the GCHAZ are displayed in Figures 12(a) and 13(a). The typical location of the fatigue crack front in the GCHAZ in these specimens is displayed in Figures 12(b) and 13(b), respectively. As described above, few fractures occurred outside the GCHAZ and some of these are presented in Figures 14 through 17.

In some specimens the cross sections prepared to examine the fracture initiation displayed subsurface cracks located in the GCHAZ, for example see Figure 18. As can be seen in this photomicrograph, the cracks are trans-granular and the fracture surface of such cracks should exhibit coarse shiny facets.

3.3 ANALYSIS OF THE CTOD RESULTS

The CTOD results are displayed in Figure 19, to show the variation with test temperature. Here the GCHAZ data are identified separately (as open points) and fracture initiation in this case mostly took place from regions with grain size of ~ 150 μm. When fracture initiation takes place outside the GCHAZ the individual locations are identified with the respective data point. It is very clear that the CTOD toughness of the GCHAZ is much lower than that of the regions outside the GCHAZ, at test temperatures above ~ -20°C. Below -20°C, the data points obtained indicate the CTOD toughness of the two regions (GCHAZ and outside) are low and similar. The CTOD transition curve of the base metal obtained from previous work (1) is also shown for comparison. When considering the 0.1 mm CTOD transition temperature, it is about

-30°C for the base metal and about 25°C for the GCHAZ; a shift of about 55°C. A similar shift is also observed in the 0.2 mm CTOD transition temperature.

3.4 CVN RESULTS

The CVN test results are presented in Table 4. Even though the notch location was nominally the same for all specimens, this data is also separated into two sets based on the fracture surface appearance, i.e., shiny coarse facets or dull gray surface; the former is considered to correspond to CVN toughness values of the GCHAZ, and the latter for the HAZ regions outside the GCHAZ. (It is difficult to determine the initiation location from a broken Charpy specimen with certainty when compared to a CTOD specimen.)

Figure 20 presents the CVN transition curves for the GCHAZ and the remainder of the HAZ. The lower toughness of the GCHAZ in relation to the HAZ outside the GCHAZ is obvious in this figure; for example, the 40 Joule transition temperature is about -20°C for the GCHAZ compared to -40°C for the region outside the GCHAZ. The shift in the 40 J transition temperature is smaller than in the 0.2 (or 0.1) mm CTOD transition temperature. This is to be expected, since in the CTOD test the fatigue crack can interact with a region in the order of grain size; on the other hand, the V-notch with a radius of 0.254 mm (0.010") cannot sample dimensions of that order.

3.5 SIGNIFICANCE OF THE RESULTS

The CTOD results demonstrate that the HAZ associated with the weld made in the WP steel has local brittle zones. Their CTOD toughness is very low as compared to that of the base steel. From previous studies (3, 7), it is clear that if a flaw were to interact with or be present in the LBZ, however improbable that might be, brittle fracture initiation is likely to occur. In such an event, the integrity of the structure depends on the crack arrest capability of the surrounding HAZ and base material.

Fortunately, the previous study showed that the crack arrest behaviour of the same HAZ, as assessed by the short crack arrest test and the NDT temperature, is very similar to that of the base material (2). In the compact crack arrest tests carried out for the heat-affected zone in the same study, it was also extremely difficult to initiate cracks in the HAZ. However, in four of the specimens (out of 19), the crack was able to propagate all the way along the HAZ, to within ≈ 12 to 14 mm of the backwall. It therefore seems that if a propagating crack is constrained to a particular critical plane in the GCHAZ, as in the plain strain compact crack arrest test, then the HAZ crack arrest toughness could be lower than that of the base material.

Overall, it seems that a fracture control plan based solely on HAZ CTOD toughness could be extremely conservative and expensive, and that one incorporating crack arrest capability could be more economical.

4.0 CONCLUSIONS

The current work led to the following conclusions:

i) CTOD testing produced low values (< 0.2 mm up to a temperature of 40°C) for the GCHAZ, thereby demonstrating the presence of LBZs. The 0.1 mm CTOD transition temperature is about 25°C.

ii) Post-test metallographic analysis showed that the low CTOD values represented fracture initiation sites located in regions where the prior austenite grain size is about 150 μm.

iii) When fractures initiate outside the GCHAZ, the CTOD's are significantly higher, at least at test temperatures > ~ -20°C.

iv) The CVN testing also produced lower toughnesses for specimens displaying coarse shiny facets (representing the GCHAZ) compared to specimens containing fine facets (representing the regions outside the GCHAZ). However, the shift in 40 J transition temperature was smaller than that in 0.1 mm CTOD transition temperature.

v) It is suggested that a fracture control plan based solely on HAZ CTOD toughness could be too conservative and expensive, and the one based on the crack arrest toughness of base materials and HAZ could be more economical.

5.0 REFERENCES

1. Malik, L., and Tomin, M., "Evaluation of Toughness of Conventional Ship Steels at Intermediate Loading Rates, and Its Implications", report submitted by Fleet Technology Limited to the Metals Technology Laboratories, CANMET, and the Canadian Coast Guard (Northern), January 1991.

2. "Characterization of the Steel and Heat-Affected Zone Used in the Wide Plate Project", report submitted by Fleet Technology Limited to the Project Manager, "Study of Wide Plate Testing of Structural Steels for Arctic Ships", April 1991.

3. Malik, L., and Pussegoda, N., "Statistical Significance of Local Brittle Zones in Heat-Affected Zones in Welded Structures", report submitted by Fleet Technology Limited to the Metals Technology Laboratories, CANMET, April 1992.

4. Towers, O.L., and Robinson, P., "Procedure for Fatigue Cracking, Fracture Toughness Testpieces, with Particular Reference to Weldments", The Welding Institute Research Bulletin, April 1982, pp. 112-120.

5. Akselsen, O.M. et. al., "Assessment and Predictions of HAZ Tensile Properties of High Strength Steel", Welding Journal, 1989, pp. 356-S to 362-S.

6. Irwin, G.R., "Linear Fracture Mechanics, Fracture Transition and Fracture Control", Eng. Frac. Mech., 1968, pp. 241-257.

7. Pussegoda, L.N. et. al., "Significance of Local Brittle Zones in Weld Heat-Affected Zones - Wide Plate Tests", International Conference of Offshore Mechanics and Arctic Engineering, Calgary, Alberta, June 7-11, 1992.

TABLES AND FIGURES

FLEET TECHNOLOGY LIMITED

Welding Procedure Data Sheet

Project No: 4025C
Specimen No:

Material Specification:
Welding Process: SAW
Manual or Machine: Machine
Position of Welding: 1G
Filler Metal Brand Name: LA75-880M Flux Dia. = 5 mm
Filler Metal Classification:
Shielding Gas: Flow Rate:
Nozzle Orifice Size:
Single or Multipass: Multipass (2 pass)
Single or Multiple Arc: Single
Heat Input Requirement (E): - 5 kJ/mm
Preheat Temperature: Take away moisture from bar
Interpass Temperature: -- --
Preheat Method:

(Indicate material thickness on drawing)

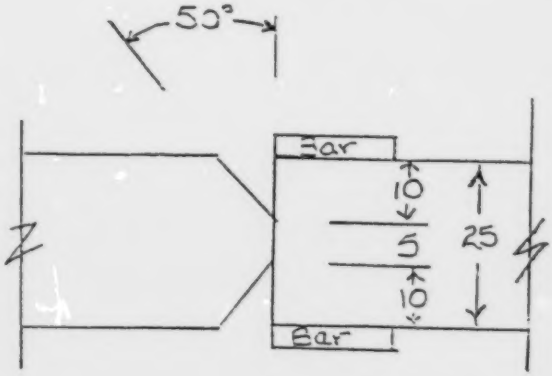

Joint Preparation

Weld Size	Side	Layer	Pass No.	Amps I	Amps Dial	WFS mm/min	WFS Dial	Volts V	Volts Dial	Travel Speed (s) mm/min	Travel Speed (s) Dial	E.S.O. mm
	1	1	1	780-805		1245		36		305		31
	2	1	1	1020-1050		1702		38		381		31

$E = \frac{I \times V \times 60}{S}$

Procedure Notes:
① Objective is to obtain a straight HAZ
② with little distortion
③
④
⑤
⑥
⑦

Procedure Application Notes:
①
②
③
④
⑤
⑥
⑦

Date:	Welder's Name:	Inspected By:	Procedure By:
January 1992	L. Thompson		

Table 1: Welding Procedure Data Sheet

Table 2: Results of Hardness Traverse Performed on Cross-Sections of the Weld

Section	Location	Vickers Hardness ($HV_{5\,kg}$)		
		Base Metal	Coarse Grain HAZ	Weld Metal
1	Subsurface	175	210	216
	Half-Thickness	177	212	214
2	Subsurface	175	210	198
	Half-Thickness	174	206	192

Table 3: CTOD Test Results

Fracture Initiation Site	Sample	Notch Location	Temp. (°C)	a/W	B (mm)	W (mm)	Yield Strength (MPa)	CTOD (mm)	Mode of Failure
GCHAZ	2.4	GCHAZ	-20	0.525	25.050	50.210	436	0.069	c
	1.19	GCHAZ	-20	0.523	24.560	49.250	436	0.063	c
	1.20	GCHAZ	-40	0.519	24.360	48.890	455	0.031	c
	1.18	GCHAZ	-40	0.507	24.600	49.090	455	0.018	c
	1.17	GCHAZ	-40	0.530	24.480	49.080	455	0.044	c
	1.9	GCHAZ	-20	0.506	24.640	49.500	436	0.068	c
	1.2	GCHAZ	0	0.511	24.790	49.570	420	0.021	c
	1.14	GCHAZ	0	0.522	24.940	50.040	420	0.053	c
	1.15	GCHAZ	0	0.525	25.050	50.090	420	0.134	c
	2.6	GCHAZ	20	0.504	24.510	49.220	406	0.105	c
	1.10	GCHAZ	20	0.504	24.800	49.600	406	0.129	c
	1.4	GCHAZ	40	0.524	24.970	50.040	394	0.199	c
	1.6	GCHAZ	46	0.505	24.810	49.890	390	0.421	u
	1.13	GCHAZ	10	0.510	24.490	48.980	412	0.006	c
	1.8	GCHAZ	10	0.509	24.990	49.990	412	0.034	c
	1.11	GCHAZ	-10	0.512	24.130	48.380	427	0.237	c
	1.5	GCHAZ	-10	0.500	25.010	50.220	427	0.043	c
	1.12	GCHAZ	10	0.502	24.520	49.120	412	0.062	c
	1.16	GCHAZ	0	0.507	24.730	49.770	420	0.110	c
	1.7	GCHAZ	-10	0.501	25.100	49.930	427	0.009	c
Outside GCHAZ	1.3	GCHAZ	20	0.497	25.040	50.070	406	0.830	m
	1.1	GCHAZ	37	0.537	24.910	49.560	395	0.924	u
	2.7	Outside GCHAZ	0	0.508	24.350	48.830	420	0.730	u
	2.8	Outside GCHAZ	10	0.515	24.510	49.410	412	0.368	u
	2.3	Outside GCHAZ	-10	0.511	24.500	49.060	427	0.528	u
	2.5	Outside GCHAZ	-40	0.506	25.330	50.770	455	0.083	c
	2.9	Outside GCHAZ	-20	0.521	24.720	49.410	436	0.057	c

Table 4: Charpy V-Notch Test Results

GCHAZ		HAZ (Outside GCHAZ)	
T (°C)	Absorbed Energy	T (°C)	Absorbed Energy
-60	9	-40	54
-30	20	-40	46
-20	50	-40	37
-20	42	-40	37
-20	37	-20	94
0	77	-20	125
-40	37	0	125
		0	140
		0	138
		10	146
		20	145
		20	130

Figure 1: A typical cross-section of the weld, displaying a large straight GCHAZ (right side) associated with the second pass. (X 2.2), Negative No. 13127.

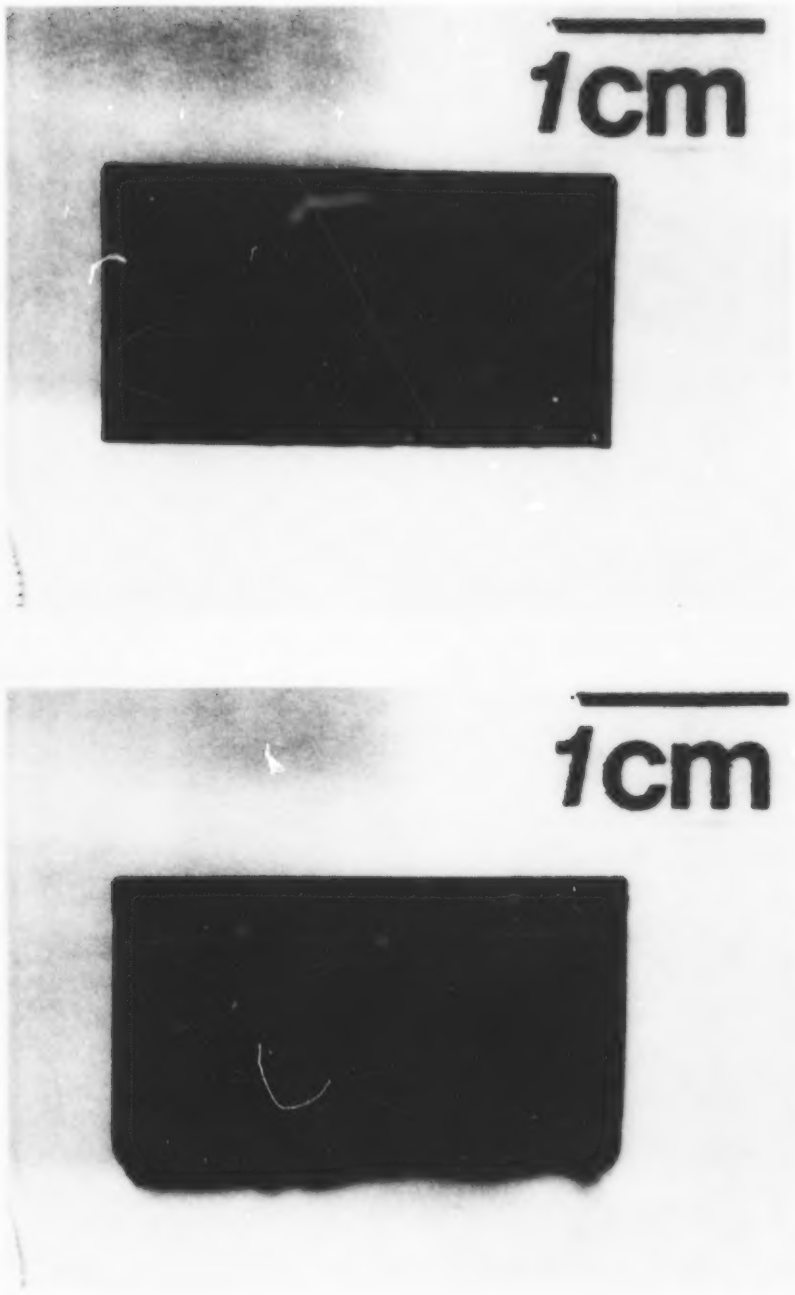

Figure 2: Macrographs of the fatigue crack front (a) and the fracture in . . tion plane (b) of CTOD specimen 1-5, (T = -10°C, δ_c = 0.043 mm). The fracture initiation region is indicated by the arrow. Negative Nos. 14003 and 14010, respectively. (Note that the orientations are reversed in the two macrographs.)

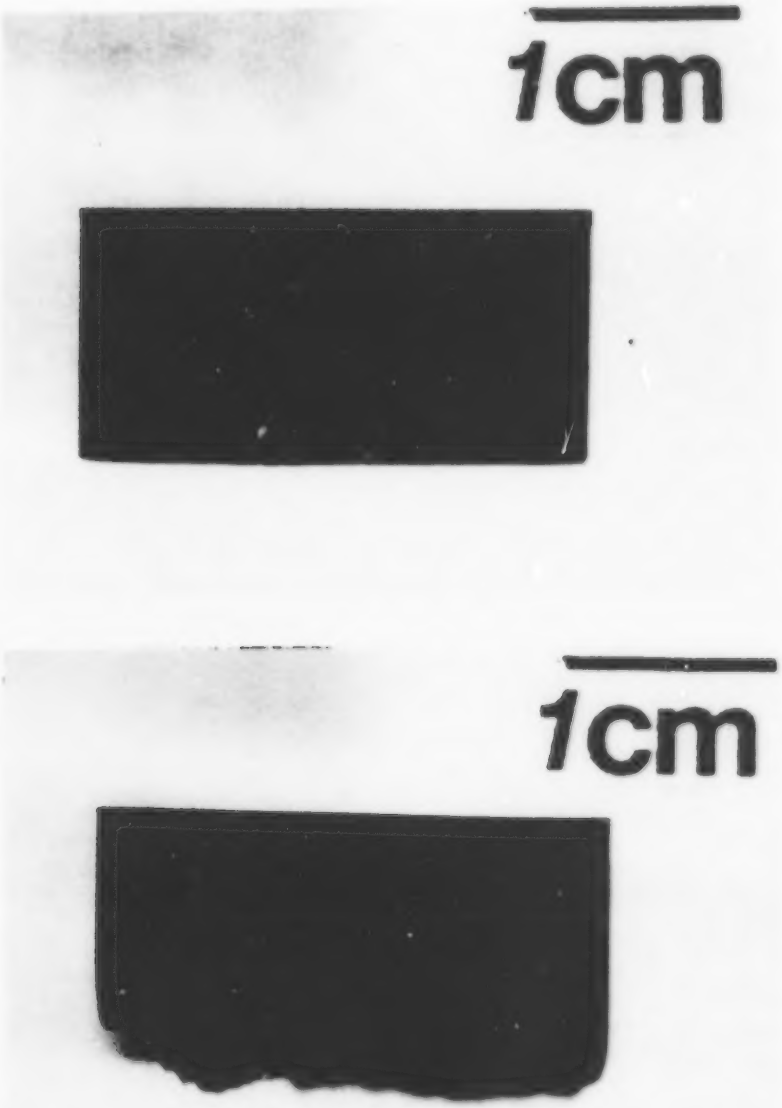

Figure 3: Macrographs of the fatigue crack front (a) and the fracture initiation plane (b) of CTOD specimen 1-14, (T = 0°C, δ_c = 0.053 mm). The fracture initiation region is indicated by the arrow. Negative Nos. 14005 and 14012, respectively. (Note that the orientations are reversed in the two macrographs.)

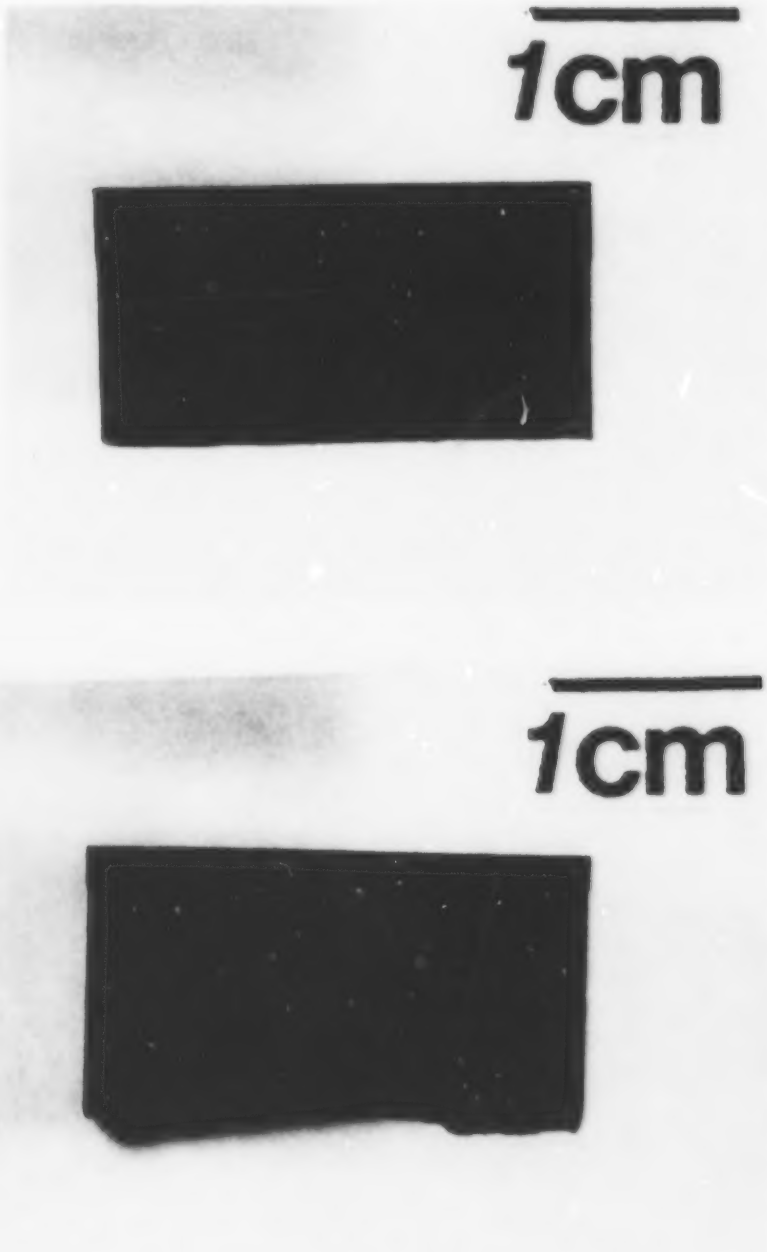

Figure 4: Macrographs of the fatigue crack front (a) and the fracture initiation plane (b) of CTOD specimen 1-20, (T = -40°C, δ_c = 0.031 mm). The fracture initiation region is indicated by the arrow. Negative Nos. 14006 and 14014, respectively. (Note that the orientations are reversed in the two macrographs.)

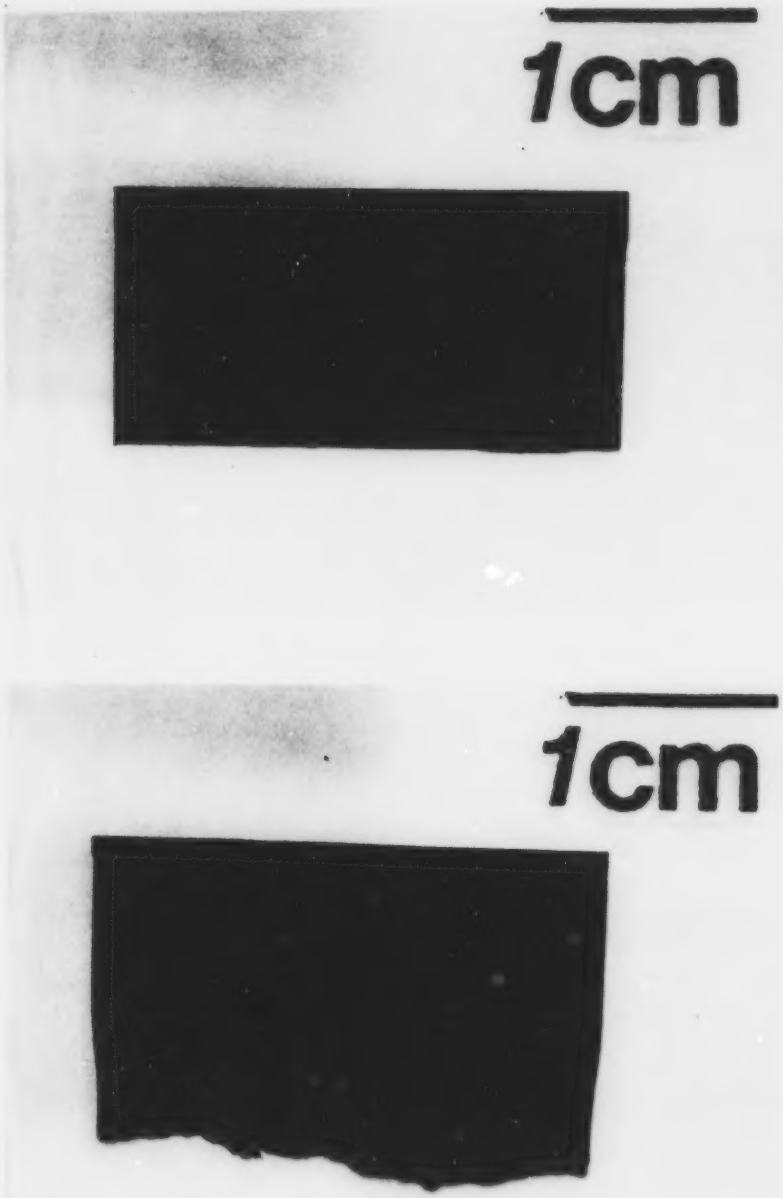

Figure 5: Macrographs of the fatigue crack front (a) and the fracture initiation plane (b) of CTOD specimen 1-3, (T = 20°C, δ_u = 0.830 mm). The fracture initiation region is indicated by the arrow. Negative Nos. 14004 and 14013, respectively. (Note that the orientations are reversed in the two macrographs.)

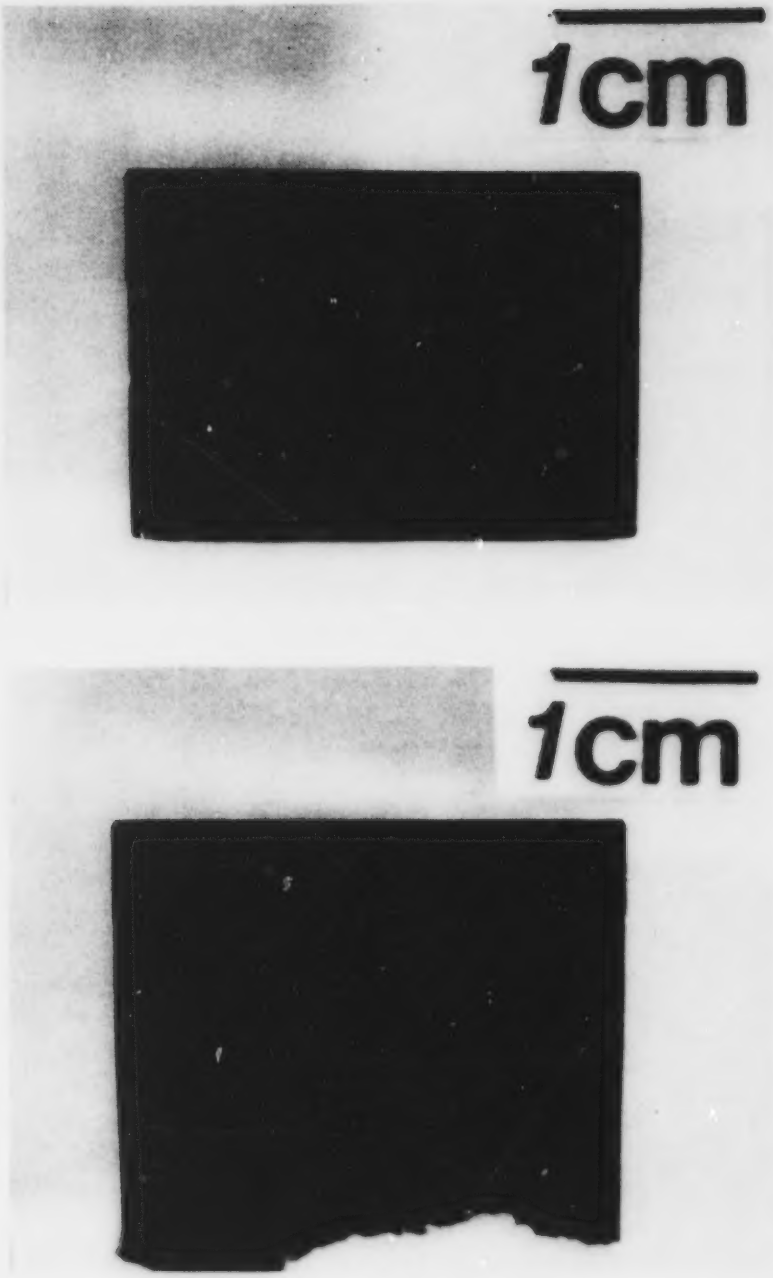

Figure 6: Macrographs of the fatigue crack front (a) and the fracture initiation plane (b) of CTOD specimen 1-1, (T = 37°C, δ_u = 0.924 mm). The fracture initiation region is indicated by the arrow. Negative Nos. 14001 and 14009, respectively. (Note that the orientations are reversed in the two macrographs.)

(a)

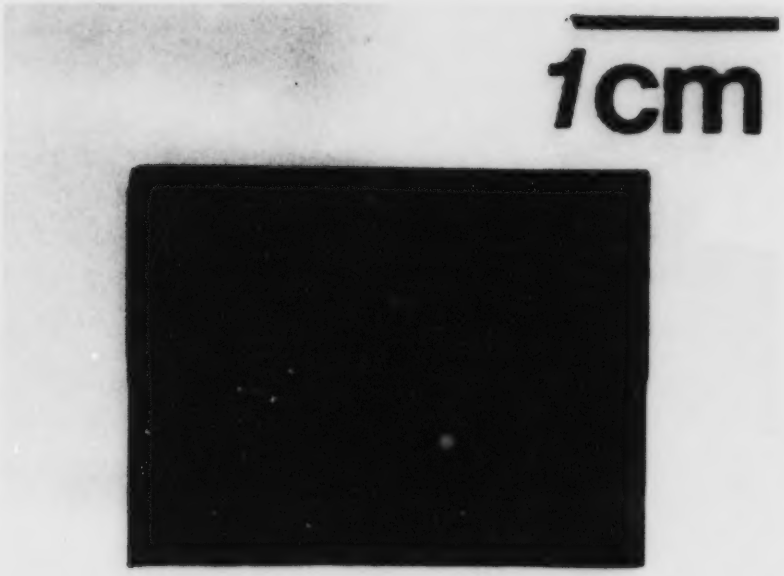

(b)

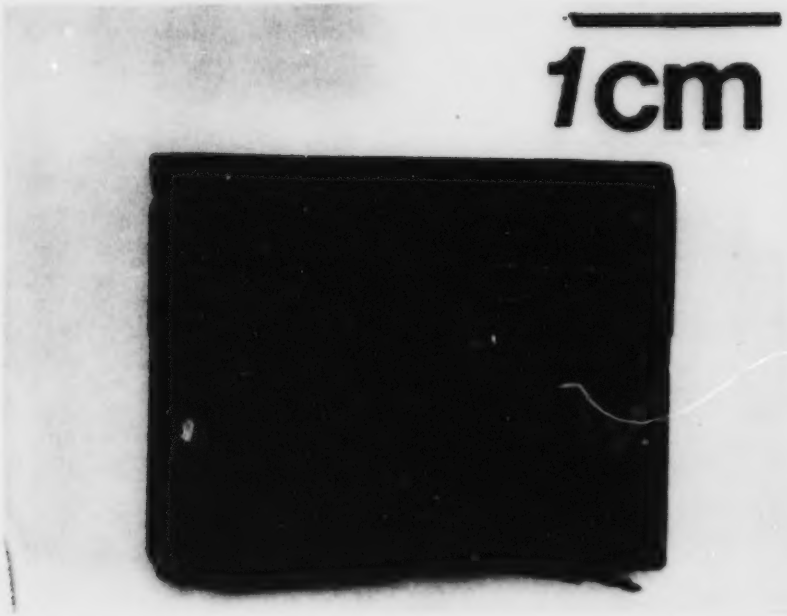

Figure 7: Macrographs of the fatigue crack front (a) and the fracture initiation plane (b) of CTOD specimen 2-5, (T = -40°C, δ_c = 0.083 mm). The fracture initiation region is indicated by the arrow. Negative Nos. 13199 and 14011, respectively. (Note that the orientations are reversed in the two macrographs.)

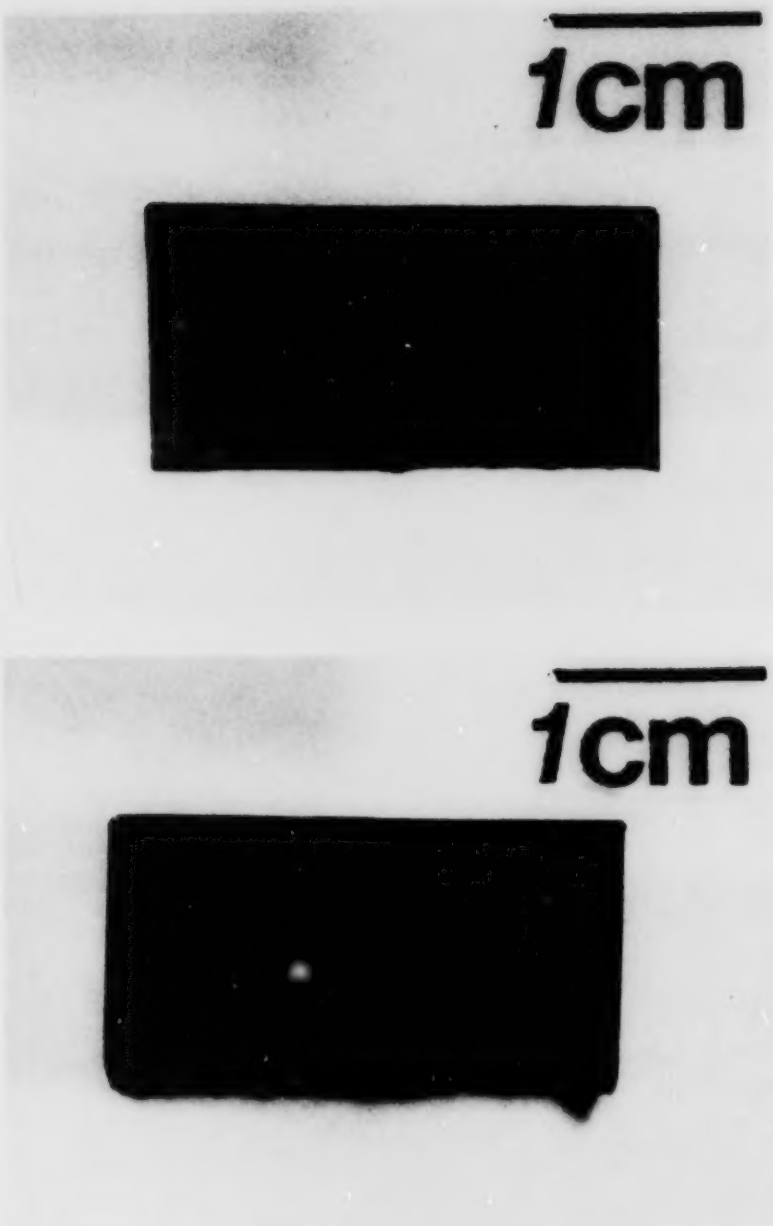

Figure 8: Macrographs of the fatigue crack front (a) and the fracture initiation plane (b) of CTOD specimen 1-8, ($T = 10°C$, $\delta_c = 0.034$ mm). The fracture initiation region is indicated by the arrow. Negative Nos. 14000 and 14015, respectively. (Note that the orientations are reversed in the two macrographs.)

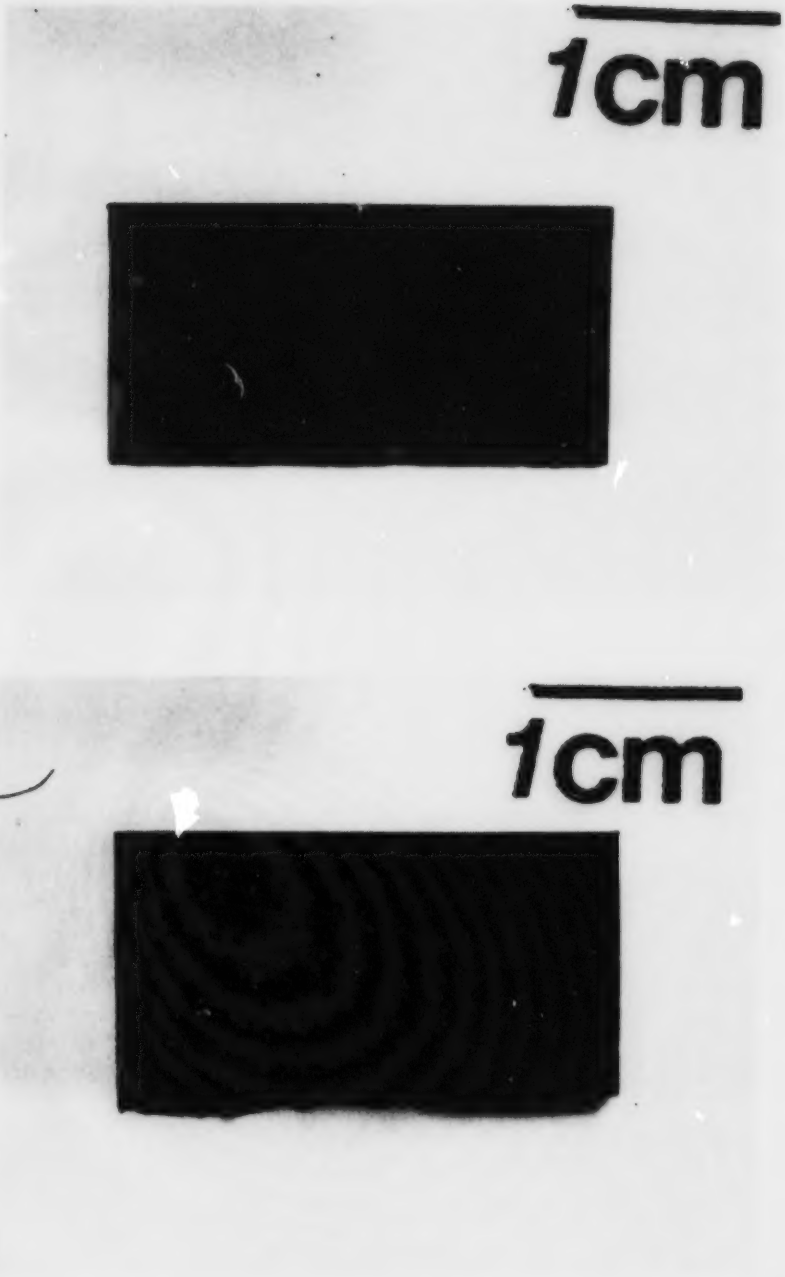

Figure 9: Macrographs of the fatigue crack front (a) and the fracture initiation plane (b) of CTOD specimen 2-6, ($T = 20°C$, $\delta_c = 0.105$ mm). The fracture initiation region is indicated by the arrow. Negative Nos. 14007 and 14018, respectively. (Note that the orientations are reversed in the two macrographs.)

(a)

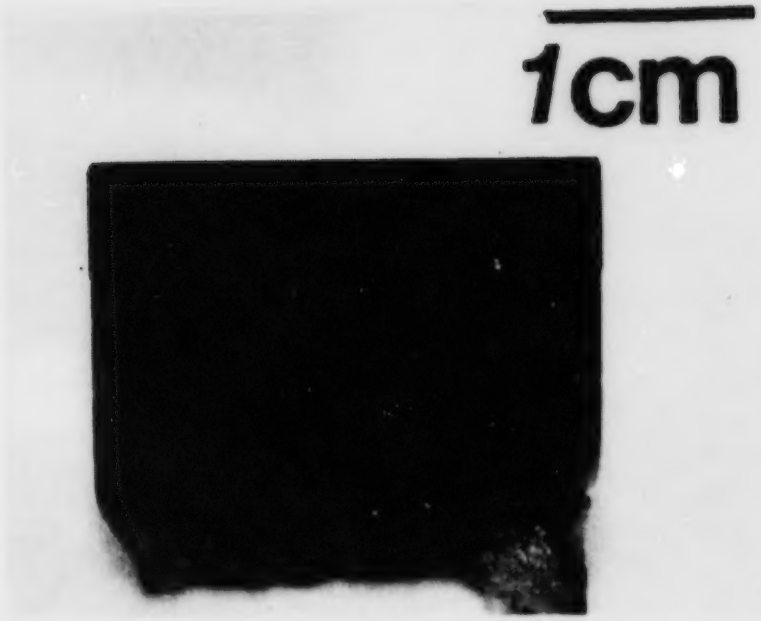

(b)

Figure 10: (a) Fracture face of specimen 1-4 (T = 40°C, δ_c = 0.199 mm) where the initiation region displays coarse facets; (b) shows the macrograph of the fracture initiation site which is almost at the fusion line. Arrows indicate the initiation site. The shiny thumbnail occurred at the "pop-in" and the dark region below is a result of ductile fracture subsequent to the pop-in. Negative Nos. 14020 and 14002, respectively.

(a)

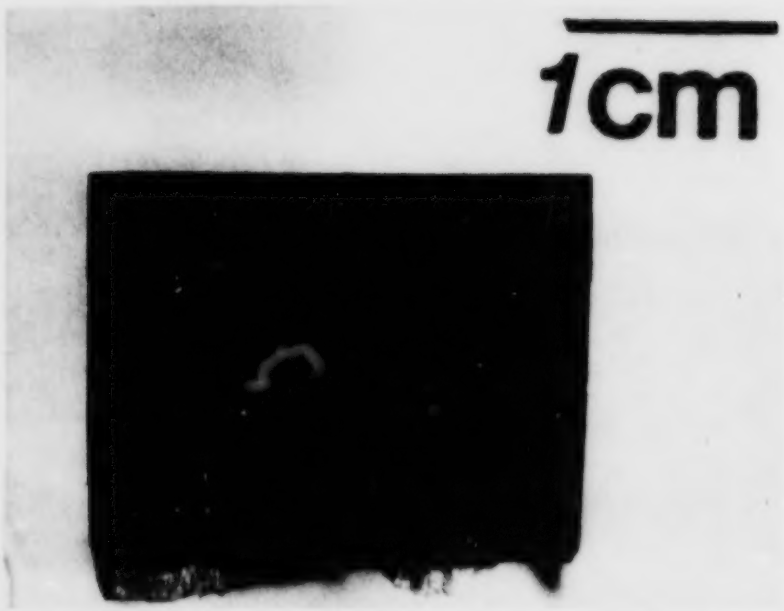

(b)

Figure 11: (a) Fracture face of specimen 2-7 (T = 0°C, δ_u = 0.730) where the initiation region displays fine facets in relation to Figure 10(a); (b) shows the macrograph of the fracture initiation site which occurs outside the GCHAZ. The bright area represents the pop-in after ductile extension, and the dark region below that is a result of ductile fracture subsequent to the pop-in. Arrows indicate the initiation sites. Negative Nos. 14019 and 14008, respectively.

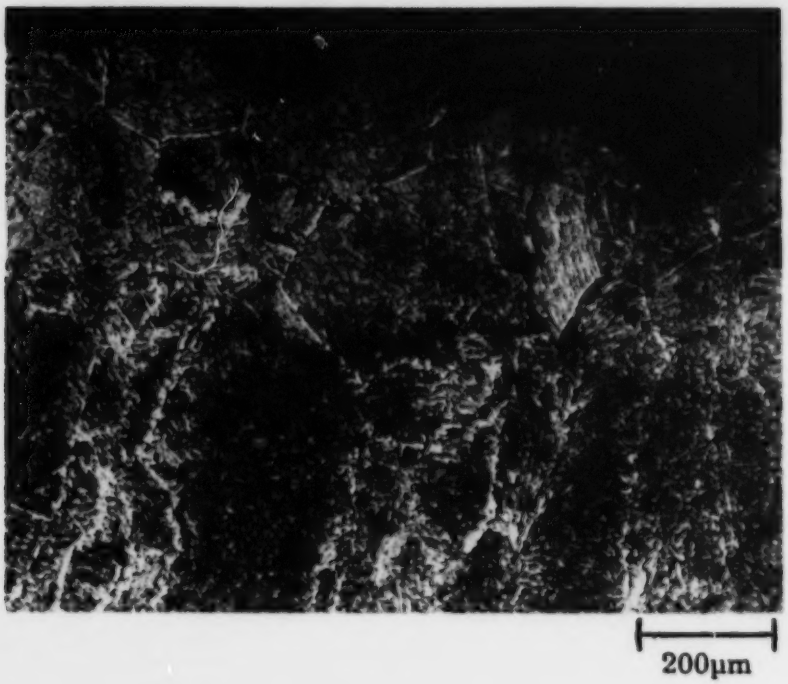

Figure 12(a): The fracture initiation region displaying the pro-eutectoid-ferrite, outlining the coarse prior austenite grains (~ 150 μm) adjacent to the fusion line. Specimen 1-14 (T = 0°C, δ_c = 0.053 mm). Negative No. 13178.

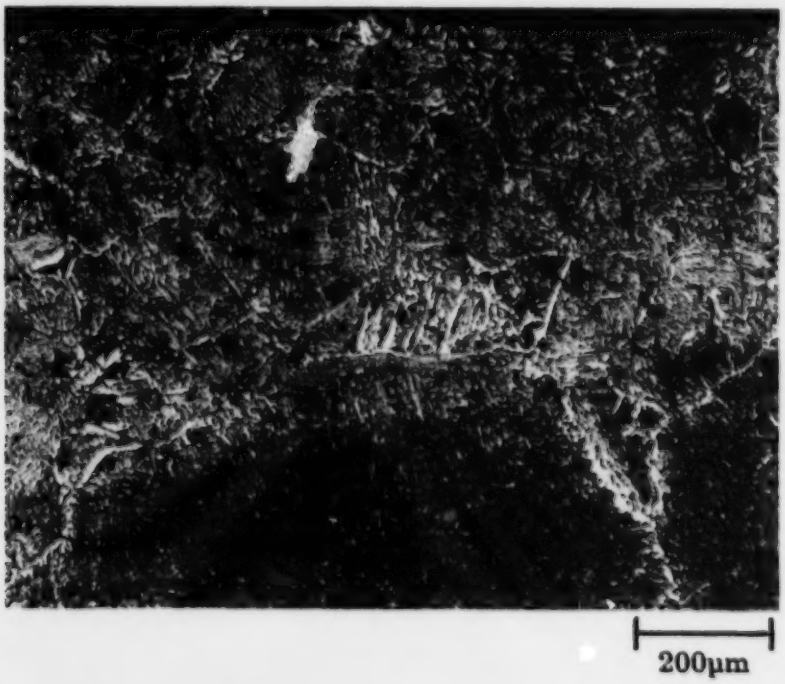

Figure 12(b): Specimen 1-14; fatigue crack front located in the GCHAZ adjacent to the fusion line. Negative No. 13177.

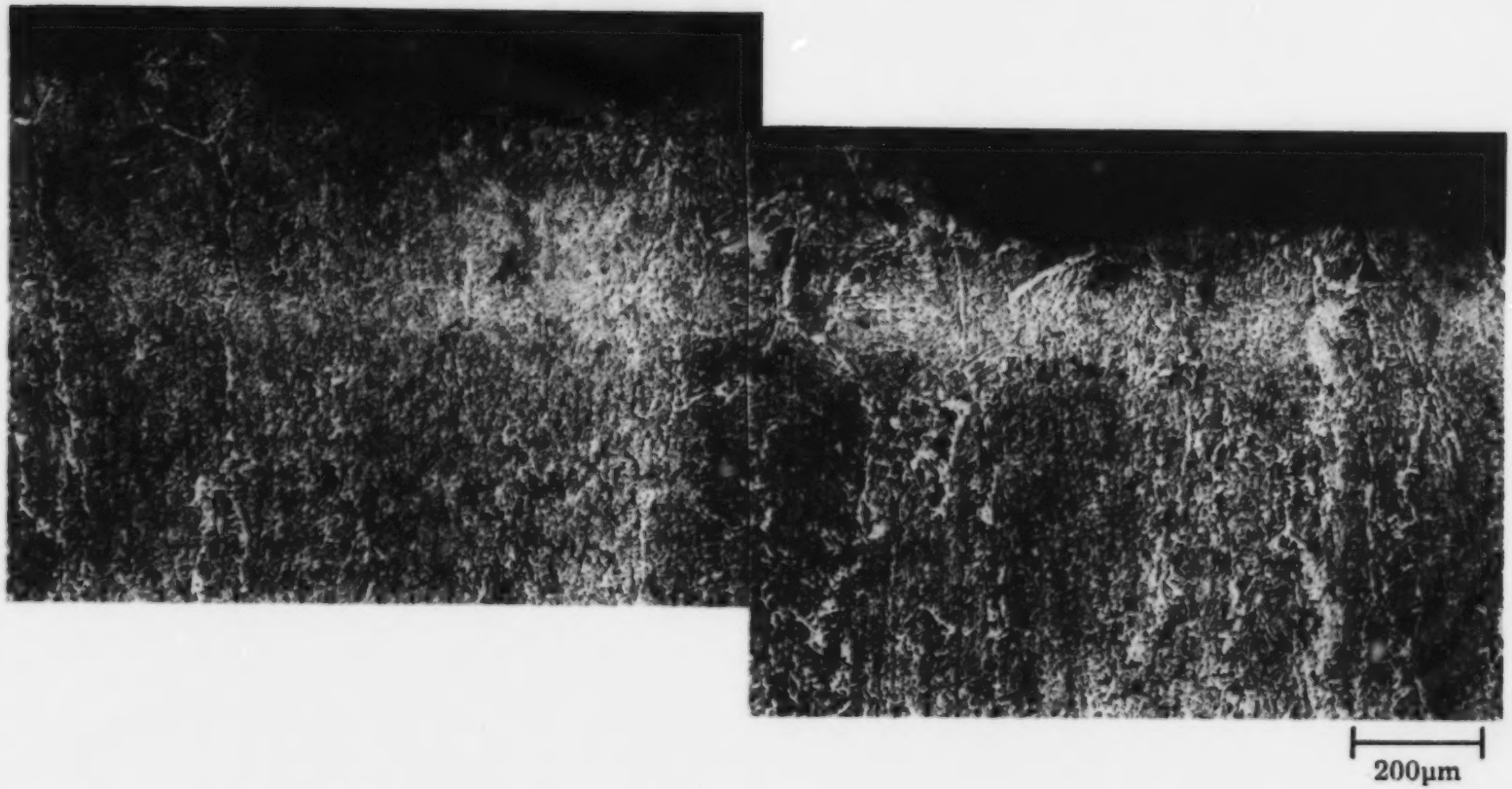

Figure 13(a): Fracture initiation region adjacent to the fusion line. Specimen 1-20 (T = -40°C, δ_c = 0.031 mm). Negative No. 13181 and 13182.

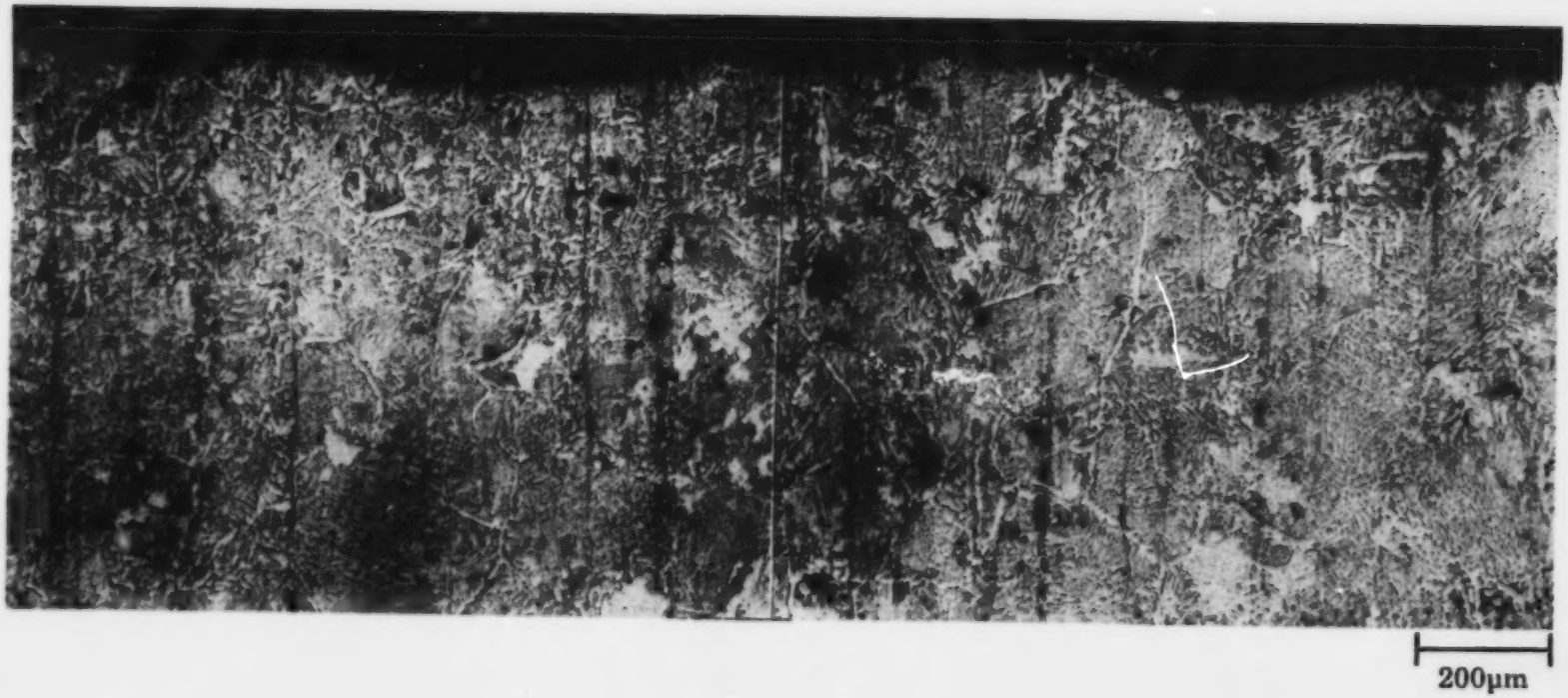

Figure 13(b): Specimen 1-20; fatigue crack front at the boundary of the GCHAZ, i.e., grain size ~ 100μm. Negative No. 13179 and 13180.

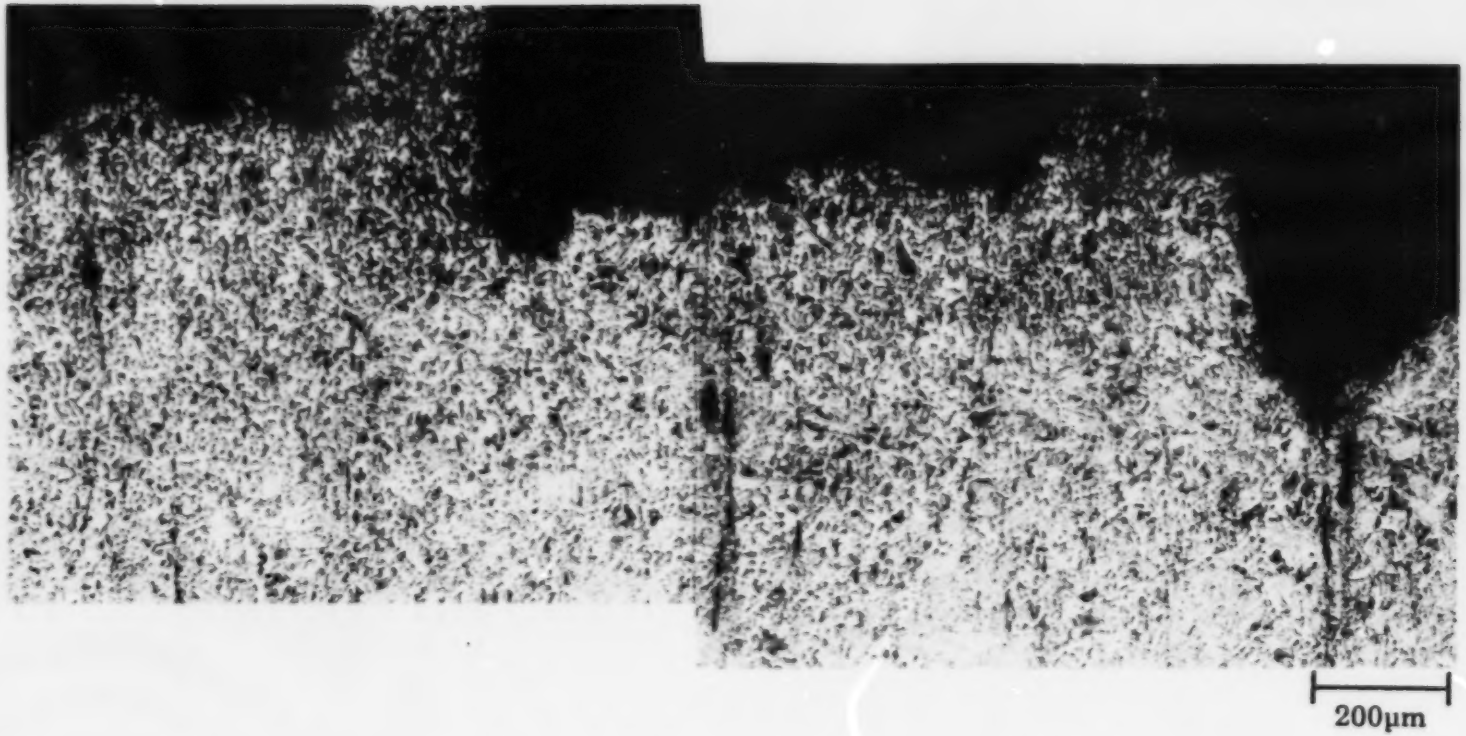

Figure 14: Fracture initiation in grain-refined HAZ (GRHAZ). Specimen 1-3, T = 20°C, δ_m = 0.830 mm. Negative No. 13194 and 13195.

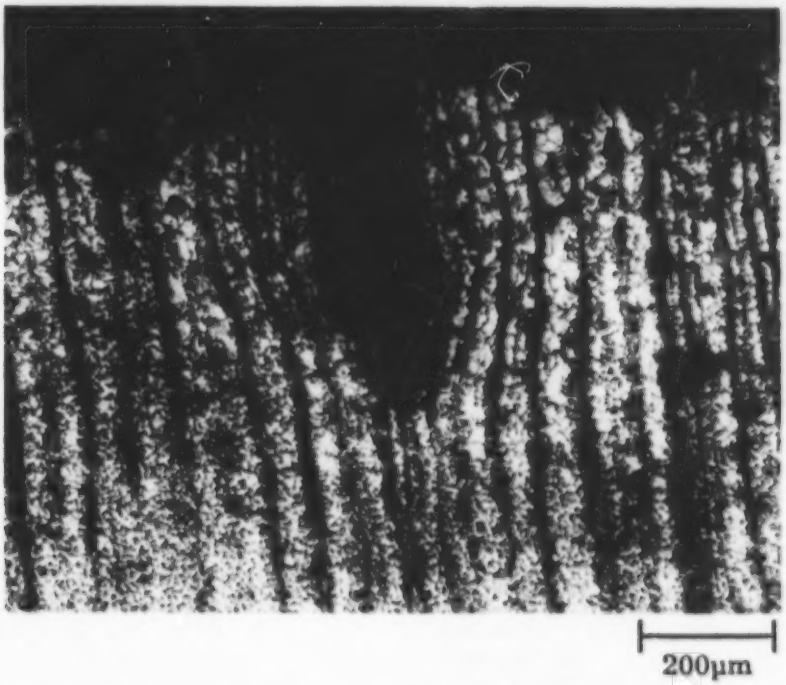

Figure 15: Fracture initiation in intercritical HAZ (ICHAZ). Specimen 2-7, T = 0°C, δ_u = 0.730 mm. Negative No. 13187.

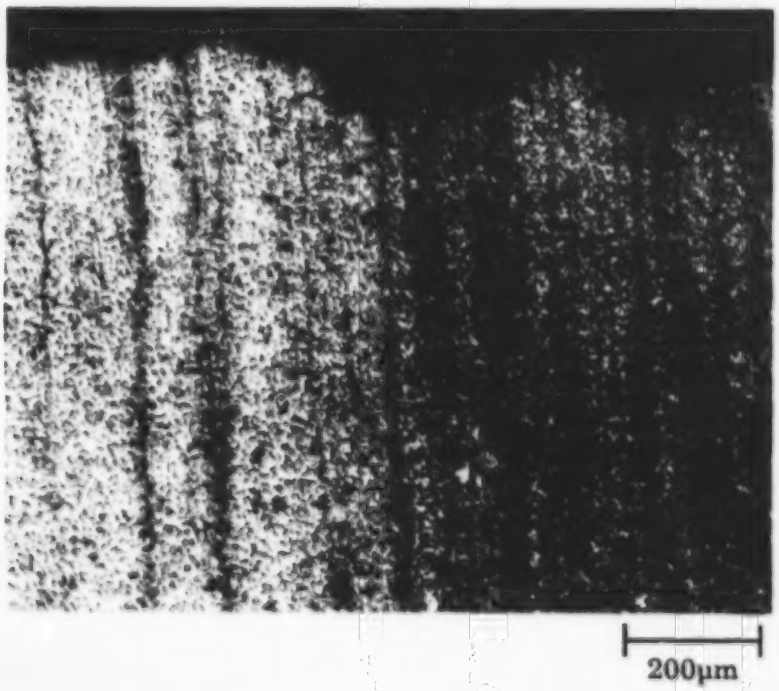

Figure 16: Fracture initiation in fine-grain HAZ (GRHAZ). Specimen 2-5, T = -40°C, δ_c = 0.083 mm. Negative No. 13192.

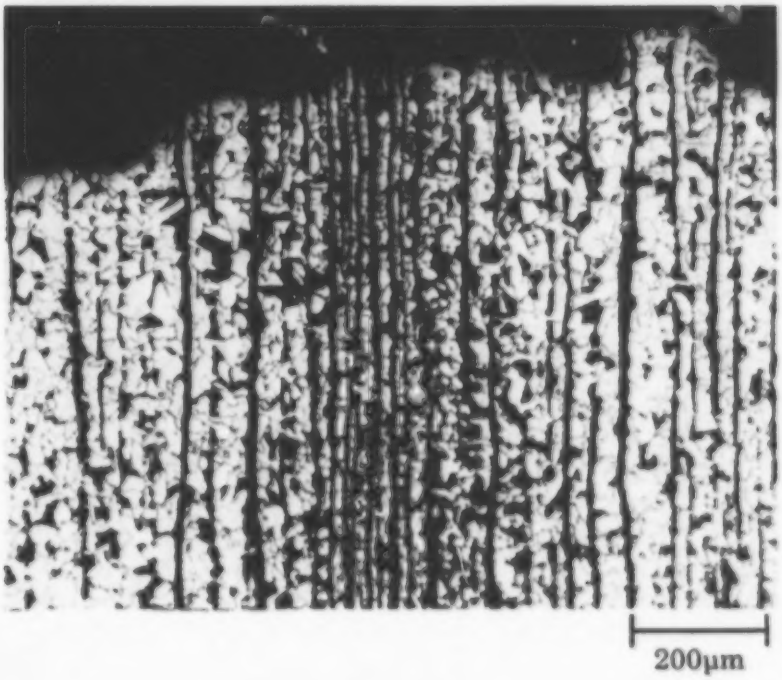

Figure 17: Fracture initiation in parent metal (PM). Specimen 2-9, T = -20°C, δ_c = 0.057 mm. Negative No. 13193.

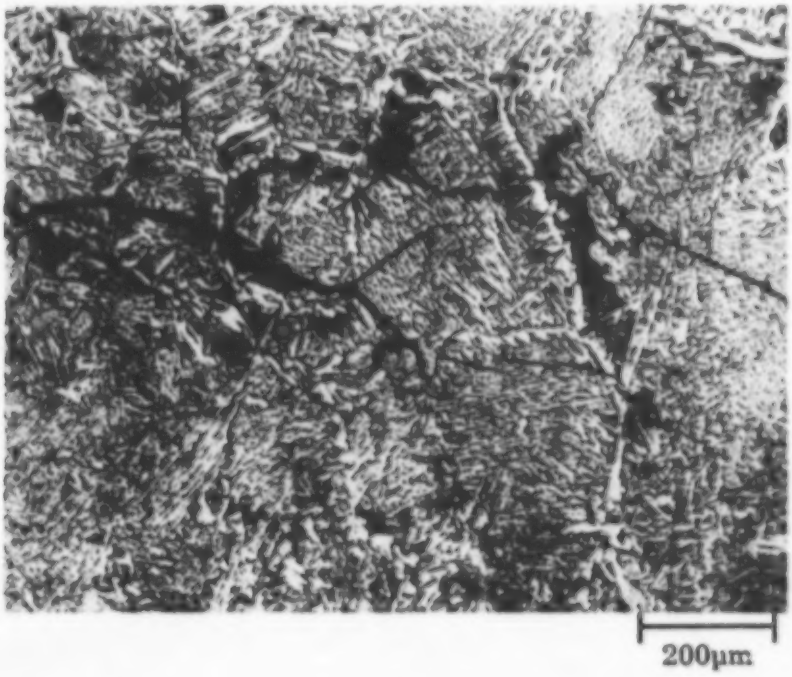

Figure 18: Subsurface transgranular cracks in GCHAZ. Specimen 2-5, T = -40°C, δ_c = 0.083 mm. Negative No. 13190.

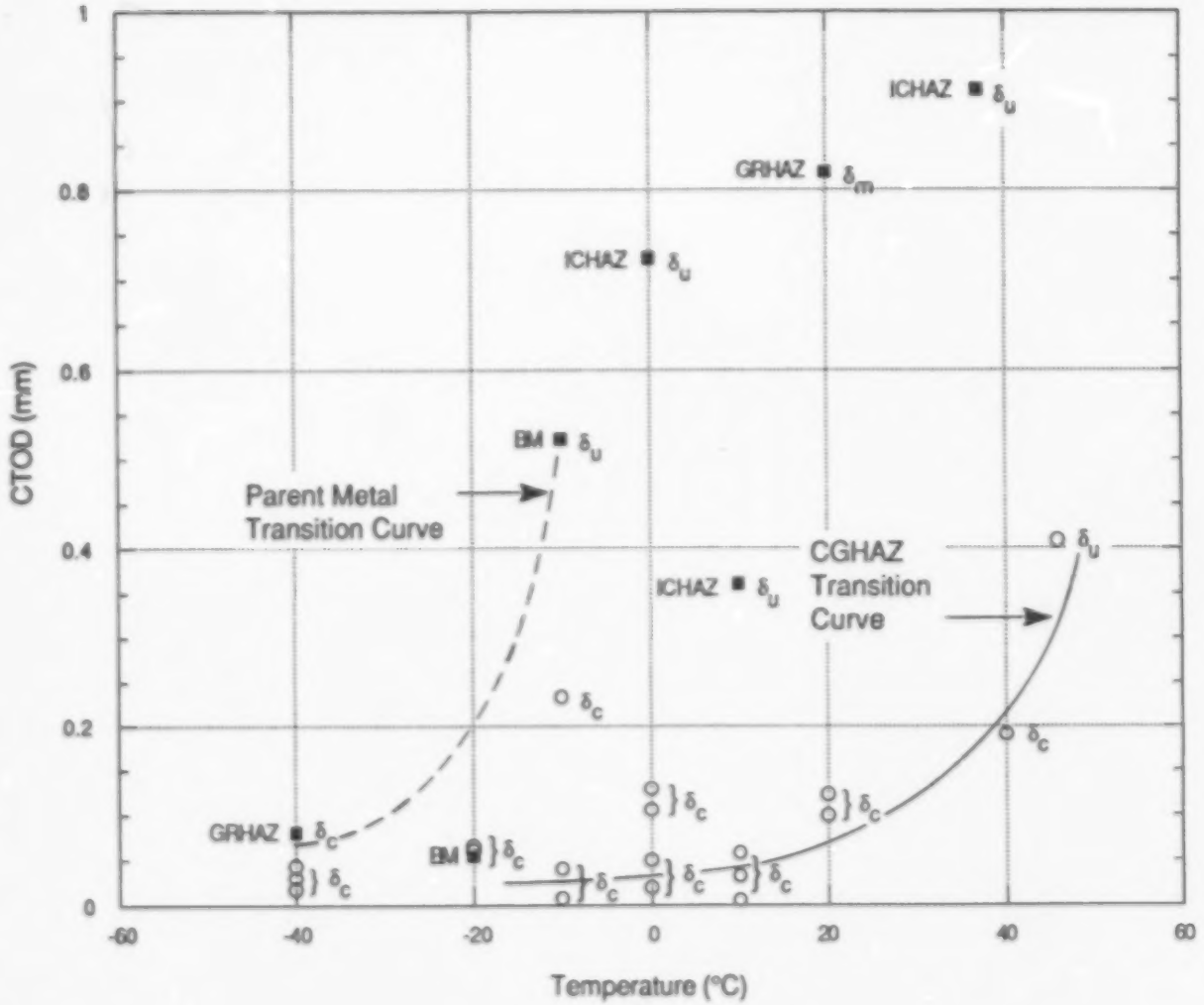

Figure 19: CTOD Results vs. Temperature. Open data points represent GCHAZ behaviour and the parent metal transition curve is obtained from previous work (1).

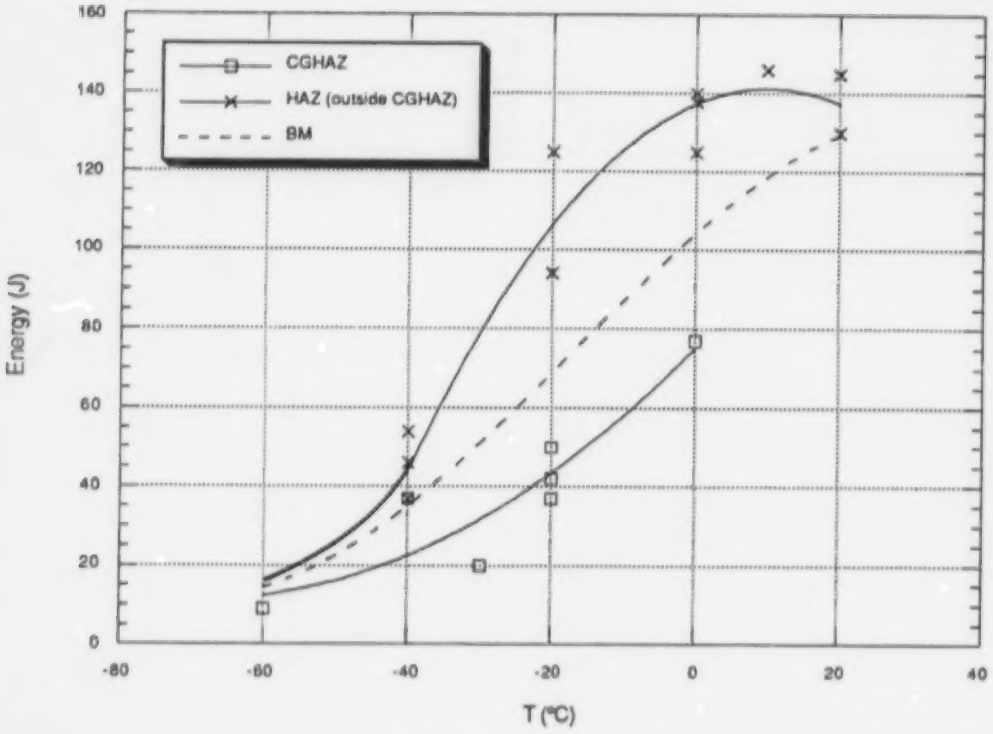

Figure 20: CVN transition curves for the GCHAZ and the HAZ outside the GCHAZ, and the base metal from previous work.